

# RESIDUAL STRESSES INDUCED BY HIGHLY REACTIVE THERMOSETS DURING HEATED RTM

Barcenas, Leonardo<sup>12</sup>, and Hubert, Pascal<sup>12\*</sup>

<sup>1</sup> Department of Mechanical Engineering, McGill University, 817 Sherbrooke Street West, Montreal, QC H3A 2K6, Canada.

<sup>2</sup> Research Centre for High Performance Polymer and Composite Systems. QC, Canada.

\* Corresponding author (pascal.hubert@mcgill.ca)

**Keywords:** *Highly reactive thermosets, residual stresses, heated RTM simulation*

## ABSTRACT

This manuscript aims to propose an integrated solution to the prediction of residual stresses and the final shape of the components manufactured with highly reactive thermosets. A highly reactive resin system (Gurit SPX26528/SPX26373) is used for this analysis. The methodology consists of simulating the residual stresses of a representative geometry using a cure hardening instantaneously linear elastic behaviour (CHILE). Curing and residual stresses simulations are performed with an integrated modeling methodology. Degree of cure gradients during heated resin transfer moulding (RTM) are accounted during the integrated method. The results are compared with a traditional sequential methodology, where the initial degree of cure gradients are neglected. It is shown that the initial degree of cure gradients have an influence on the final shape of the part. A novel strategy is then expected to simulate residual stresses using highly reactive thermosets accounting for material transformations from the beginning of the process.

## 1 INTRODUCTION

Highly reactive thermosets are expected to boost the manufacturing of composite materials at large scale production rates. The transportation industry aims to implement more composite structures in order to reduce the overall weight of the vehicles and reduce gas emissions. Among the manufacturing processes, compression resin transfer moulding (CRTM) is one of the most promising processes for large scale production [1]. The high reactivity of these resins creates manufacturing and quality challenges for moulded parts, parts design, and tooling. The existing process simulation tools must be modified to take into account the dynamic behaviour of these resins and new physical models of these materials must be developed. Dimensional distortion on composite materials is inherently produced by the residual stresses generated by the manufacturing process conditions [2]. The final shape of the composite component depends on non-uniform resin flow, tooling effects, shrinkage, and cure gradients [3]. The cure gradients are more extensive with the use highly reactive thermosets. These gradients produce a non-uniform evolution of the mechanical properties of the composite structure, and distortion is expected from these degree of cure gradients. The first objective is to consider and couple the mechanical properties of the resin involved during residual stresses simulation (cure kinetics, coefficient of thermal expansion, cure shrinkage, and thermo-viscoelasticity). A second objective is to implement a sequential strategy for simulation, which will be compared with an integrated method, where the degree of cure gradient from injection is accounted for the residual stresses and deformation simulation.

## 2 MATERIALS

The matrix used for the process simulation is a fast-curing resin system developed by Gurit. The resin name is Gurit SPX26528, and the hardener is Gurit SPX26373, with a mix ratio of 100:25 part per weight. This material was characterized using a differential scanning calorimeter for the cure kinetics and glass transition temperature model, a thermomechanical analyzer for the coefficient of thermal expansion model, a rheometer for the shrinkage model, and a dynamic mechanical analyzer for the thermo-viscoelastic model. The properties are summarized on the following sub-sections. The preform used for this analysis is a Texonic TG-15-N NCS E-Glass with a volume fraction of 0.4. Aluminum 6060 is used for the cure and stress-deformation simulation. The material properties of the preform are taken from COMPRO database [4-8].

### 2.1 Cure Kinetics

A combined catalytic and autocatalytic model is used for the cure kinetics of the Gurit resin described in Equations 1 and 2 [9]. The cure kinetics is complemented with a glass transition temperature model described by Equation 3 [10].

$$\frac{d\alpha}{dt} = (K_1 + K_2\alpha^m)(1 - \alpha)^n \quad (1)$$

$$K_i = A_i \exp\left(\frac{-E_{a_i}}{RT}\right) \quad (2)$$

$$T_g = T_{g0} + \frac{\lambda\alpha(T_{g\infty} - T_{g0})}{1 - (1 - \lambda)\alpha} \quad (3)$$

where  $\alpha$  is the degree of cure,  $\frac{d\alpha}{dt}$  is the cure rate,  $E_{a_i}$  is the activation energy ( $E_{a_1}=52160$  J/mol and  $E_{a_2}=43750$  J/mol).  $A_i$ ,  $m$ , and  $n$  are fitting constants ( $A_1=53090$ ,  $A_2=12280$ ,  $m=0.1$  and  $n=1.69$ ). The resin system has a total exothermic energy of  $H_f=410$  J/g. Figure 1 shows the cure kinetics model agreement with the experimental data acquired on a DSC for different isothermal tests.  $T_{g0}=-47$  °C and  $T_{g\infty}=140$  °C are the initial and final glass transition temperatures respectively.  $\lambda$  is a fitting constant with a value of 0.5455. Figure 2 shows the glass transition temperature model.

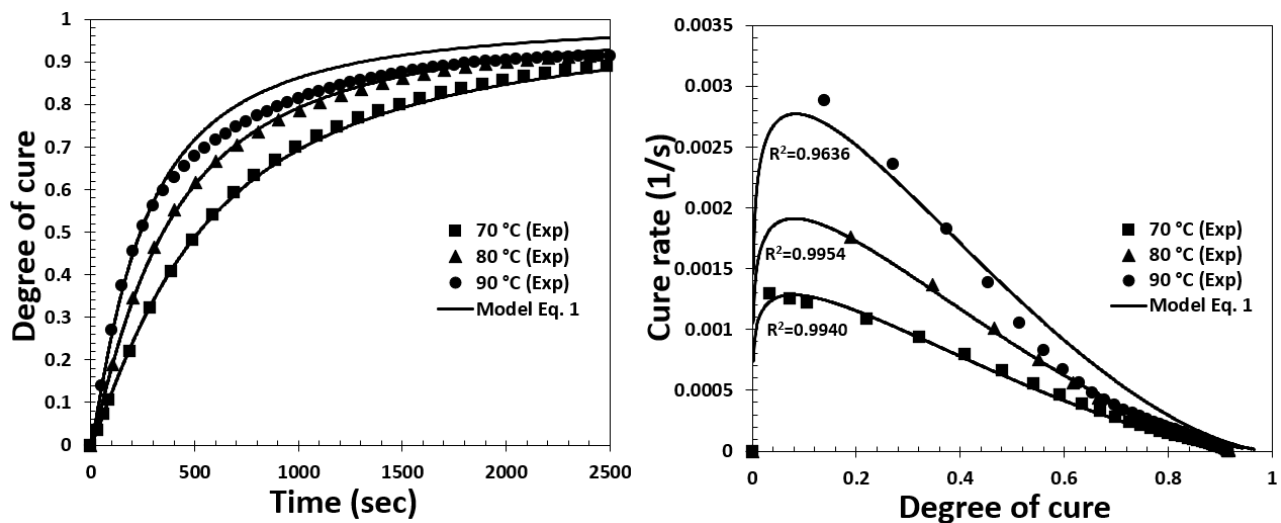


Figure 1 Cure kinetics model for the Gurit resin system.

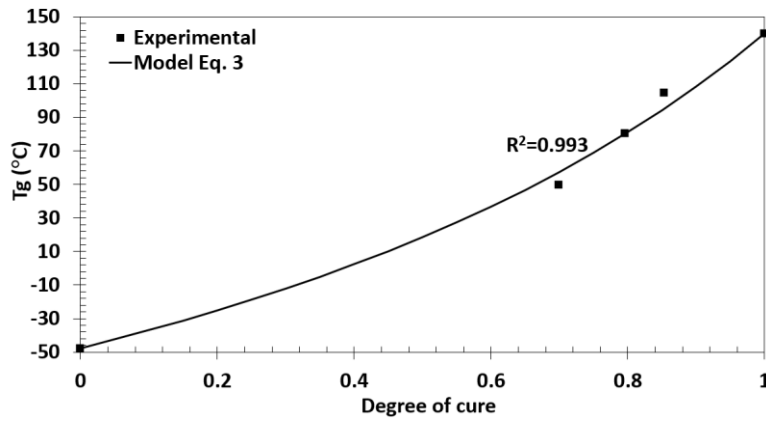


Figure 2 Glass transition temperature model for the Gurit resin system.

## 2.2 Coefficient of Thermal Expansion

The resin coefficient of thermal expansion is modelled as a piecewise function (Equation 4) based on the work of Prasaty a et al [11]. It describes a temperature-dependent glassy coefficient of thermal expansion (CTE) and a second-order polynomial transition from the rubbery and glassy CTE.

$$CTE = \begin{cases} CTE_{rub} & T_{C1} < T^* \\ C_2 + C_3 T^* + C_4 T^{*2} & T_{C2} < T^* < T_{C1} \\ CTE_{glass} + CTE_{alpha}(T^* - T_{C2}) & T^* < T_{C2} \end{cases} \quad (4)$$

$$T^* = T - T_g \quad (5)$$

where  $CTE_{rub}=1.9E-4 \text{ C}^{-1}$  and  $CTE_{glass}=9.0E-5 \text{ C}^{-1}$  are the coefficient of thermal expansion at the rubbery and glass state.  $C_2=1.614E-4 \text{ C}^{-1}$ ,  $C_3=2.857E-6 \text{ C}^{-2}$ , and  $C_4=0 \text{ C}^{-3}$  are coefficients for the quadratic transition from rubbery to glassy state of the resin.  $CTE_{alpha}=4.0E-7 \text{ C}^{-2}$  is the slope of the function during the glassy state. Figure 3 shows the model compared to the experimental data.  $T_{C1}=10 \text{ }^\circ\text{C}$  and  $T_{C2}=-25^\circ\text{C}$  are the temperature limits of transition from rubbery to glass state.

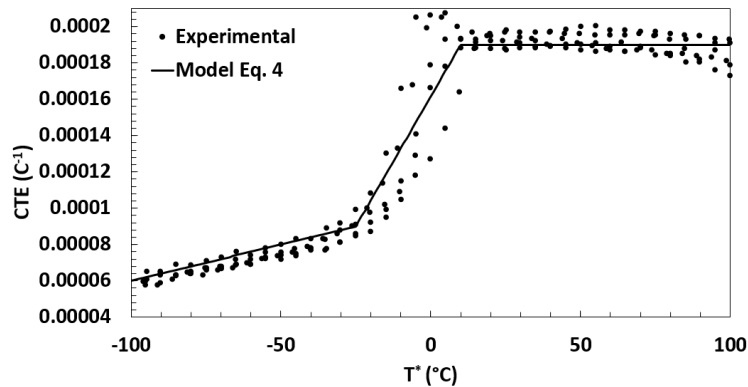


Figure 3 Coefficient of thermal expansion model for the Gurit resin system.

### 2.3 Cure Shrinkage

The resin cure shrinkage model was described by Johnson [12]. Equation 6 is the shrinkage defined by a piecewise function. It is assumed that there is no shrinkage below the gel point. Then a quadratic function is implemented until reaching a maximum value.

$$V_r^S = \begin{cases} 0 & \alpha < \alpha_{C1} \\ A\alpha_S + (V_r^{S\infty})\alpha_S^2 & \alpha_{C2} \leq \alpha < \alpha_{C2} \\ V_r^{S\infty} & \alpha \geq \alpha_{C2} \end{cases} \quad (6)$$

$$\alpha_S = \frac{\alpha - \alpha_{C1}}{\alpha_{C2} - \alpha_{C1}} \quad (7)$$

where  $\alpha_{C1}=0.78$  and  $\alpha_{C2}=0.93$  are the degree of cure limits where the shrinkage occurs.  $V_r^{S\infty}=0.29$  is the maximum cure shrinkage and  $A=0.15$  is a fitting parameter. Figure 4 shows the comparison of the shrinkage model with the experimental data.

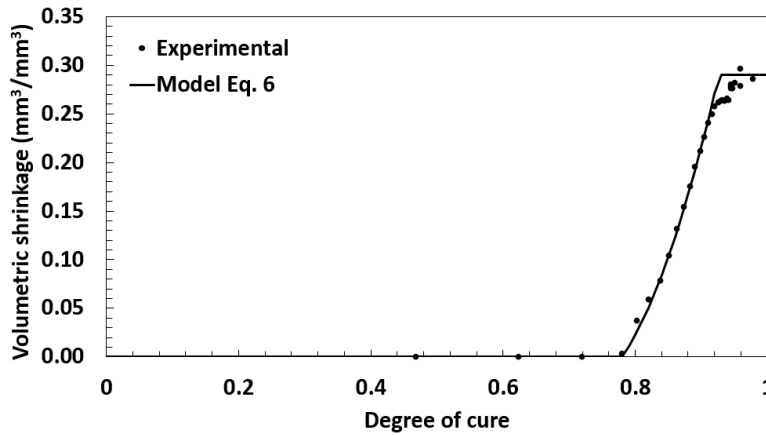


Figure 4 Shrinkage model for the Gurit resin system.

### 2.4 Modulus

The resin modulus model used in this work was described by Khoun [13]. This model describes a cure hardening instantaneously linear elastic behaviour (CHILE). Equation 8 is the resin modulus defined by a piecewise function. It is considered that the modulus is very low before  $\alpha_{gel}=0.78$ , and a minimum value of  $E_{r,min}=0.1$  MPa is assumed for computational stability. There is assumed a constant modulus  $E_1=3500$  MPa at  $T^*$  lower than  $T_1=-110$  °C. A linear behaviour is then defined from  $T_1$  to  $T_2=-13$  °C and the modulus decreases up to  $E_2=2011$  MPa. The modulus decreases linearly up to  $E_3=638.4$  MPa from  $T_2$  to  $T_3=-0.45$  °C. An exponential function is defined from  $T_3$  to  $T_4=19$  °C with the coefficients  $A=6E8$  and  $k=0.1573$ . A constant modulus  $E_4=30$  MPa is assumed at  $T^*$  higher than  $T_4$ . Figure 5 shows the comparison of the resin modulus model (CHILE) with the experimental data.

$$E_r = \begin{cases} E_{r_{min}} & \alpha < \alpha_{gel} \\ E_1 & T^* < T_1 \\ E_2 + (E_1 - E_2) \left( \frac{T^* - T_2}{T_1 - T_2} \right) & T_1 < T^* < T_2 \\ E_3 + (E_2 - E_3) \left( \frac{T^* - T_3}{T_2 - T_3} \right) & T_2 < T^* < T_3 \\ Ae^{-kT^*} & T_3 < T^* < T_4 \\ E_4 & T^* > T_4 \end{cases} \quad (8)$$

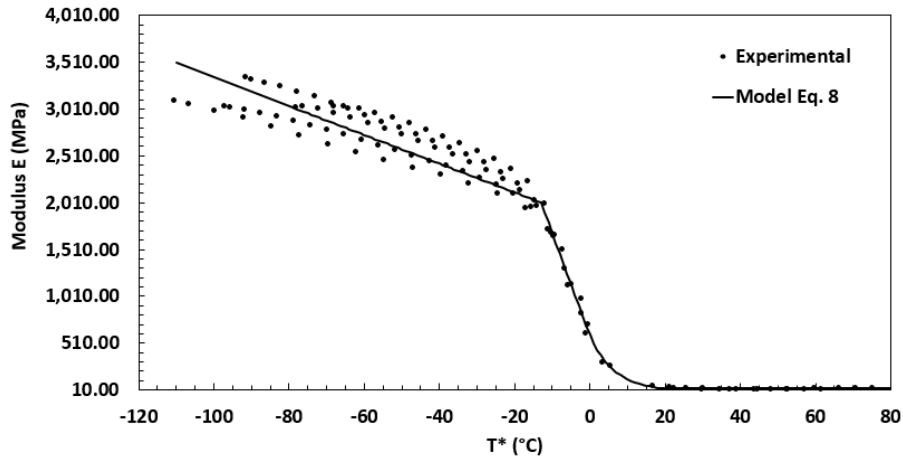


Figure 5 Cure hardening instantaneously linear elastic behaviour model for the Gurit resin system.

### 3 SIMULATION METHODOLOGY

Current simulation tools for heated RTM modelling analyze the filling and the curing separately because for aerospace slow curing resins the polymerization is slow enough such that not many changes occur during the impregnation stage. This approach is referred as the sequential method, which was first implemented by Loos and Springer and further used by other authors [14]. For highly reactive resins, the sequential approach can be improved considering that the fast polymerization affects key properties of the resin such viscosity, driving the impregnation of the fibres [15]. Furthermore, the exothermic reaction releases energy at a higher rate, thus generating high thermal gradients that can be an important source of residual stresses [16]. Finally, the degree of cure is not uniform on the part with higher polymerization state on the resin that is first in contact with the mould, which has been identified as another source of residual stresses [17].

PAM-RTM is a computational software based on the finite volumes method that simulate the resin flow through the preform. Thermal boundary conditions and cure kinetics of the resin can be implemented to compute the resin viscosity during the injection stage. In order to couple the PAM-RTM injection simulation to the residual stresses computation, the final degree of cure profile can be exported from PAM-RTM as an initial state for the stress-deformation analysis performed in COMPRO (Convergent Manufacturing Technologies). COMPRO is coupled with ABAQUS to update the mechanical properties of the resin as the degree of cure changes during the thermal process cycle.

This integrated method accounts for the non-uniform evolution of the mechanical properties, the chemical shrinkage, and the coefficient of thermal expansion variation. In COMPRO, the resin thermo-viscoelastic properties can be approximated as a cure hardening instantaneously linear elastic approach (CHILE). In this method, an uncured resin modulus is assigned below a lower bound temperature and glass transition temperature. A fully cured resin modulus is defined above an upper temperature bound and glass transition temperature. Temperature and glass transition temperature rule of mixture is therefore used for the resin for modulus development. The main advantage of using a CHILE approach is the computational time reduction, but this compromises the accuracy of the final results [18].

## 4 CASE STUDY

A circular corner laminate was used as a case study. The 10 plies laminate defined as  $[0,90,0,90,0]_s$  has an inner radius of 5 cm with a total thickness of 5 mm. The fibre volume fraction is 0.4. Figure 6 shows the boundary conditions applied on PAM-RTM for a heated process at 120 °C. A room temperature resin at constant flow injection is adjusted to let the resin flow for at least 2 minutes, which is enough to reach a maximum degree of cure of 0.68. Figure 7 shows the final degree of cure gradient which varies from 0 at the injection port up to 0.68 at the vent edge.

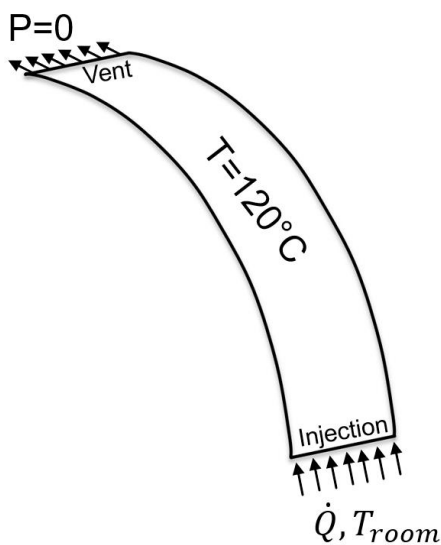


Figure 6 Boundary conditions on PAM-RTM.

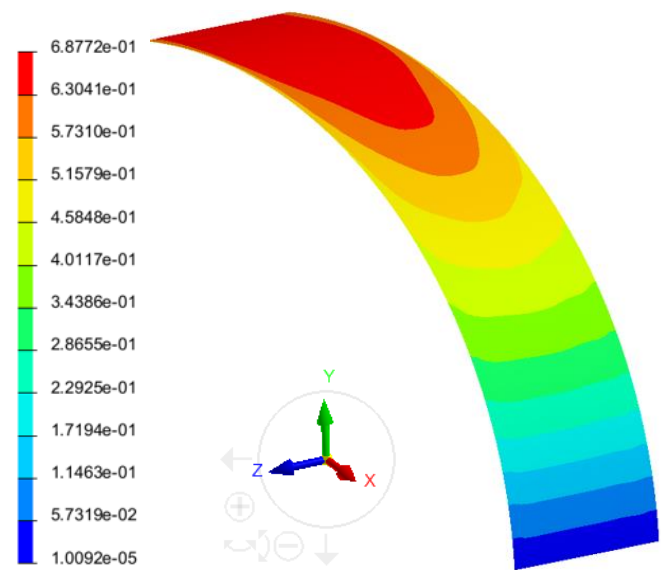


Figure 7 PAM-RTM result. Degree of cure after full impregnation.

A small representative cross-section of the corner is used for the curing and stress-deformation analysis in Abaqus. Standard 3D stress quadratic elements (C3D20) were used for the composite and the mould. One element per layer was assigned for the composite, with a total thickness of 10 elements. A global size of 1 mm was used in the rest of the model. Figure 8 shows the isothermal cure cycle at 120 °C for 15 minutes. Then the part was released and cooled down for 10 minutes. Thus, the stress and deformation simulation was divided in two simulation steps: Step 1 for the cure cycle isothermal temperature hold and Step 2 for release of the part and cool down. Figure 9 shows the thermo-mechanical boundary conditions for Step 1. A constant temperature was set on the outer surface of the mould. Heat exchange with the environment was allowed through the thickness of the mould ( $q_1''$ ). The mould was mechanically locked. A surface-to-surface contact interaction was defined between the mould and the composite allowing separation after contact. Figure 10 shows the thermo-mechanical boundary conditions for Step 2. Heat

exchange with the environment was defined on the outer surfaces to cool down ( $q_2''$ ). One edge is mechanically locked in order to allow free relaxation of the part.

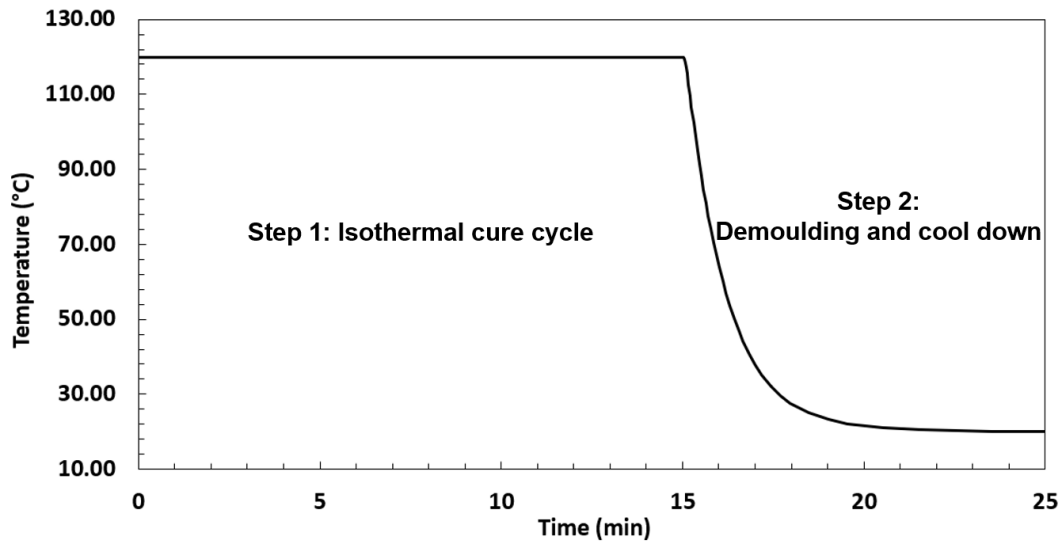


Figure 8 Isothermal cure cycle at 120 °C for 15 minutes on Step 1. Demoulding and cool down for 10 minutes on Step 2.

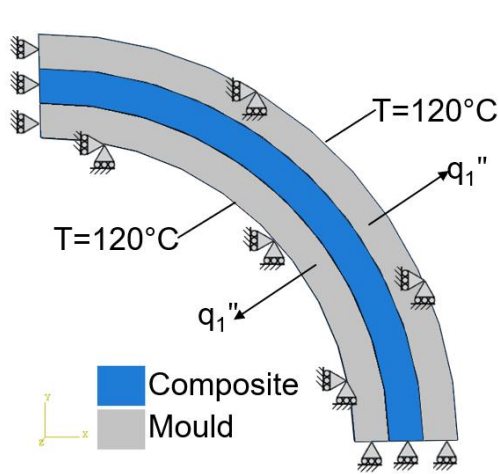


Figure 9 Themo-mechanical boundary conditions during the isothermal cure cycle (Step 1).

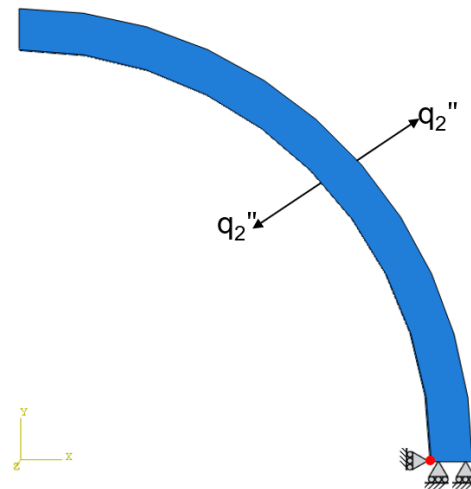


Figure 10 Themo-mechanical boundary conditions during the cool down (Step 2).

A case was defined with a global degree of cure of 0.001 as shown in Figure 11 (a) (referred as sequential method). The degree of cure gradient resulting from PAM-RTM simulation was mapped as initial condition for the second case as shown in Figure 11 (b) (referred as integrated method).

The most critical stresses occur at the end of the cure cycle. Figure 12 shows the stresses through the 11 direction, which is defined as the mould flow direction. The inner surface of the composite does not lose contact with the lower mould, while the outer surface separates from the upper mould due the cure shrinkage. Higher magnitude compressive stresses are seen on the outer ply of the composite corner. Figure 12 (a) shows that the stresses vary

with thickness but are constant through 11 direction. The degree of cure gradient defined on the integrated method generates a variation on the residual stresses through 11 direction as seen on Figure 12 (b). The higher values on stresses are located at the injection region, where the minimum value of degree of cure was assigned as initial condition. The stresses decrease on the outer layer with a difference of 44 MPa. The same behaviour is observed for the inner layer with a difference of 40 MPa. This variation is not observed on the core layer. The constant stresses observed on the sequential method have a similar magnitude to the stresses observed on half of the corner observed for the integrated method. These results suggest an influence of the degree of cure gradient for the mechanical properties evolution of the resin, which generates a variation on the the residual stresses.

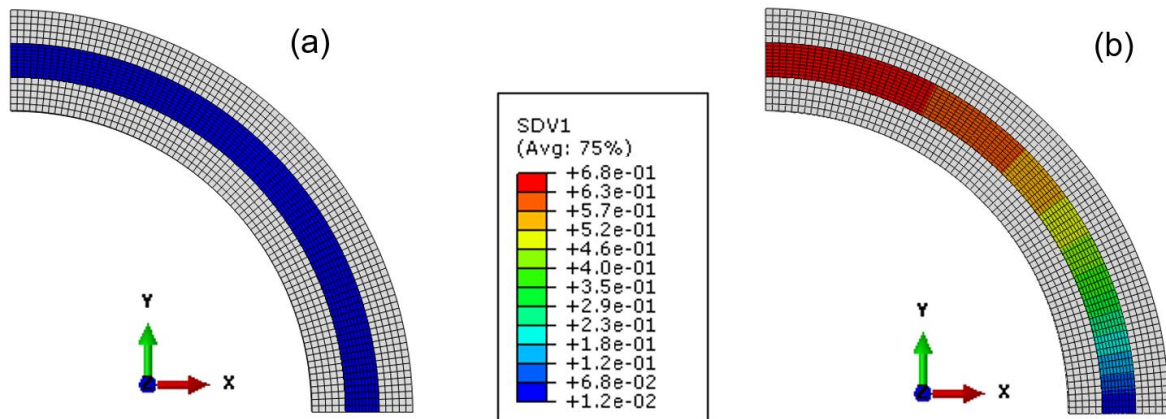


Figure 11 Initial degree of cure state on Abaqus simulations. (a) Uniform degree of cure of 0.001 (sequential method). (b) Degree of cure gradient from 0.001 to 0.68 (integrated method)

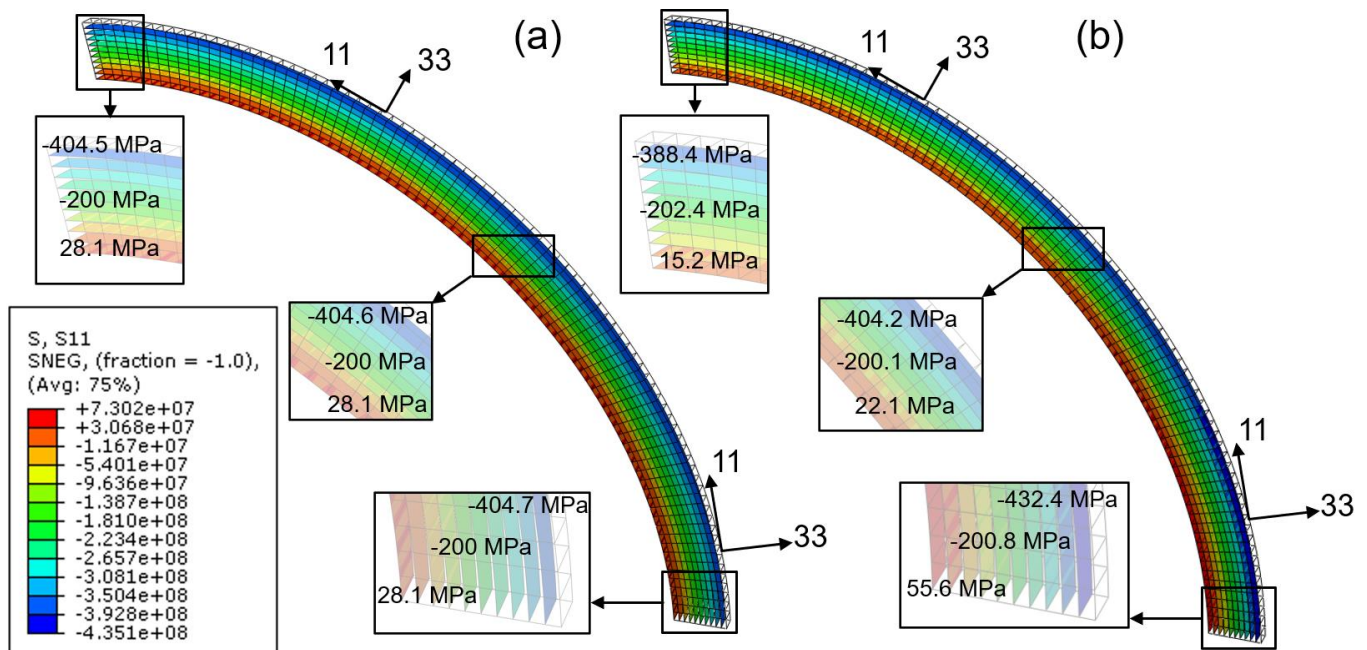


Figure 12 Residual stresses in 11 direction at the end of Step 1. (a) Sequential method. (b) Integrated method. Units in Pa.

Figure 13 shows the final shape of the corner after release, cool down and stress relaxation. Figure 13 (a) shows a deviation of  $16.04^\circ$  from the  $90^\circ$  corner for the sequential method. Furthermore, the final residual stresses after stress relaxation decreased to  $-34$  MPa on the inner layer,  $-60$  MPa on the core layer and  $-77$  MPa on the outer layer. Figure 13 (b) suggest a higher deformation of the corner with a difference of  $0.06^\circ$  with respect to the sequential method. This small variation may lead to more significant deviations on larger and more complex parts. Moreover, the variation the stresses remain on the part after stress relaxation. The final residual stress varies from  $-25$  to  $-39$  MPa for the inner layer,  $-53$  to  $-60$  MPa for the core layer, and  $-72$  to  $-82$  MPa for the outer layer.

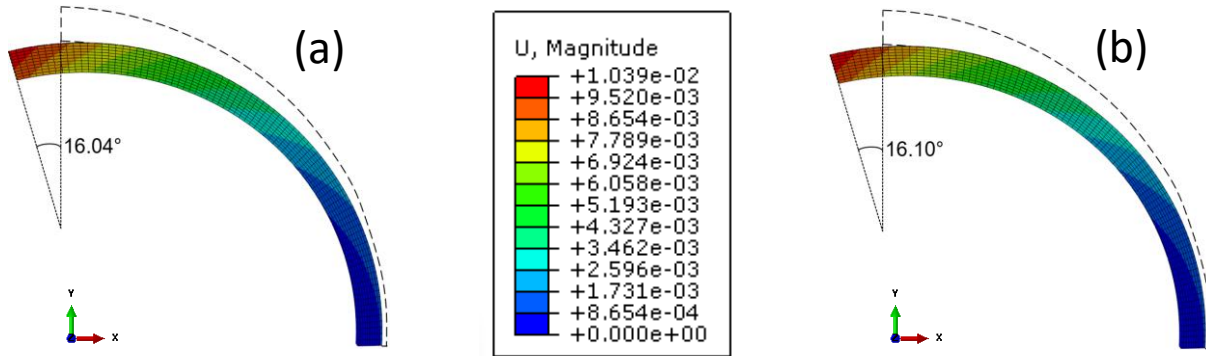


Figure 13 Final deformation after cooling down at Step 2. (a) Sequential method. (b) Integrated method. Units in m.

## 5 CONCLUSIONS

A simulation methodology was proposed for the stress-deformation analysis of laminates produced by compression resin transfer moulding. An integrated approach considered the non-uniform development of mechanical properties of the resin caused by the initial degree of cure gradients. These gradients are caused by the high reactivity of the resin when it is processed on a heated resin transfer moulding process. The results suggested an influence of the degree of cure gradient on the residual stresses and the final shape of the part. Further work should be addressed to implement a thermo-viscoelastic model for more accuracy on the final deformation predictions. An experimental work is required to verify and validate the material models and process simulation. An extensive work on the influence of the residual stress gradients should be performed for material performance analysis after manufacturing, since the mechanical properties could be compromised by the highly reactivity of these kind of resins.

## 6 ACKNOWLEDGMENTS

The authors gratefully acknowledge the financial support provided by the Natural Sciences and Engineering Research Council of Canada (NSERC), PRIMA Quebec, Texonic Inc and IND Experts. The authors would like to thank Loleï Khoun and Paul Trudeau for the technical advices. Acknowledgments to the McGill Structures and Composite Materials Laboratory members, specially to Siddharth Sarojini-Narayana and our research assistant Lucie Riffard.

## 7 REFERENCES

- [1] L. Khoun and P. Trudeau. "SNAP RTM: A cost-effective compression-RTM variant to manufacture composite component for transportation applications". *Automotive composites conference and exhibition 2018*, Novi, MI, USA, 2018.
- [2] Q. Zhu, P.H. Geubelle, M. Li and C.L. Tucker. "Dimensional accuracy of set composites: simulation of process-induced residual stresses". *Journal of composite materials*. Vol. 35, No. 24, pp 2171-2205, 2001.
- [3] A. Johnston, R. Vaziri, and A. Poursartip. "A plane strain model for process-induced deformation of laminated composite structures". *Journal of composite materials*, Vol. 35, No. 16, pp 1435-1469, 2001.
- [4] B.D. Agarwal, L.J. Broutman and K. Chandrashekhara. "*Analysis and performance of fiber composites*". 3rd edition, Wiley, 2006.
- [5] A.K. Kaw. "*Mechanics of composite materials*". 2nd edition, CRC Press, 2005.
- [6] M. Kinsella, D. Murray, D. Crane, J. Mancinelli and M. Kranjc. "Mechanical properties of polymeric composites reinforced with high strength glass fibers". *33rd International SAMPE technical conference*, Seattle, WA, USA, 2001.
- [7] F.T. Wallenberger, J.C. Watson and H. Li. "Glass fibers". *ASM International Composites Handbook*. Vol. 21, 2001.
- [8] <http://www.azom.com/properties.aspx?ArticleID=764>. Retrieved on march 31st 2022.
- [9] M.R. Kamal. "Thermoset characterization for moldability analysis". *Polymer engineering and science*, Vol. 14, No. 3, pp 231-239, 1974.
- [10] A.T. DiBenedetto. "Prediction of the glass transition temperature of polymers: A model based on the principle of corresponding states". *Journal of polymer science part B: polymer physics*, Vol. 25, No. 9, pp 1949-1969, 1987.
- [11] P. Prasatya, G.B. McKenna and S.L. Simon. "A viscoelastic model for predicting isotropic residual stresses in thermosetting materials: effects of processing parameters". *Journal of composite materials*, Vol. 35, No. 10, pp 826-848, 2001.
- [12] A.A. Johnston. "An integrated model of the development of process-induced deformation in autoclave processing of composite structures". *University of British Columbia*, Metals and Materials Engineering, Ph.D. Thesis, 1997.
- [13] L. Khoun. "Process-induced stresses and deformations in woven composites manufactured by resin transfer moulding". *McGill University*, Mechanical Engineering, Ph.D. Thesis, 2009.
- [14] A.C. Loos and G.S. Springer. "Curing of epoxy matrix composites". *Journal of composite materials*, Vol. 17, No. 2, pp 135-169, 1983.
- [15] E. Ruiz, F. Trochu and R. Gauvin. "Internal stresses and warpage of thin composite parts manufactured by RTM". *Advanced composite letters*, Vol. 13, No. 1, pp 49-57, 2004.
- [16] T.J. Chapman, J.W. Gillespie J.R, R.B. Pipes, J.-A.E. Manson and J.C. Seferis. "Prediction of process-induced residual stresses in thermoplastic composites". *Journal of composite materials*, Vol. 24, No. 6, pp 616-643, 1990.
- [17] J.-L. Bailleul, V. Sobotka, D. Delaunay and Y. Jarny. "Inverse algorithm for optimal processing of composite materials". *Composites part a: applied science and manufacturing*, Vol. 34, No. 8, pp 695-708, 2003.
- [18] N. Zobeiry, R. Vaziri and A. Poursartip. "Computationally efficient pseudo-viscoelastic models for evaluation of residual stresses in thermoset polymer composites during cure". *Composites part a: applied science and manufacturing*, Vol. 41, No. 2, pp 247-526, 2010.